Available online at www.sciencedirect.com
ScienceDirect
Ceramics International 38 (2012) 327–332
CERAMICS INTERNATIONAL
www.elsevier.com/locate/ceramint

Creep behavior modeling of silica fume containing Al_2O_3–MgO refractory castables

A.G. Tomba Martinez [a], A.P. Luz [b,*], M.A.L. Braulio [b], V.C. Pandolfelli [b]

[a] Materials Science and Technology Research Institute (INTEMA), Ceramics Division, Av. Juan B. Justo 4302, (7600) Mar del Plata, Argentina
[b] Federal University of São Carlos - Materials Engineering Department, Rod. Washington Luiz, km 235, São Carlos - SP, C.P. 676, CEP 13565-905, Brazil

Received 23 June 2011; accepted 7 July 2011
Available online 18th July 2011

Abstract

Alumina–magnesia refractory castables usually present silica fume in their compositions, due to their ability to induce better flowability and to compensate the expansion related to the *in situ* spinel formation. In this paper, four compositions containing distinct silica fume content (0–1 wt%) were designed and analyzed by creep resistance and hot mechanical strength. The θ-projection concept coupled with the thermodynamic simulations were used in order to predict the creep behavior and to identify the main mechanism leading to the deformation of the samples. Based on the collected results, a linear correlation between the creep parameters (θ_i) and the silica fume content was attained by analyzing the experimental data, resulting in reliable data and the likelihood to simulate the performance of other compositions in the same system. Moreover, particle sliding assisted by viscous flow was suggested as the dominant creep mechanism in the studied castables.

Keywords: C. Creep; Spinel containing castables; θ-Projection concept; Thermodynamic simulation

1. Introduction

Spinel containing castables are usually applied in secondary steelmaking vessels due to their outstanding chemical and thermo-mechanical properties [1]. The reaction between Al_2O_3 and MgO at temperatures above 1100 °C leads to *in situ* spinel ($MgAl_2O_4$) formation, resulting in a volumetric expansion of the refractory and, consequently, better performance due to the compressive thermal stresses generated [2]. Nevertheless, an exceeded expansion could also give rise to microcracking and affect the corrosion resistance of these materials. Therefore, there is widespread interest to find out alternative ways to master the expansion of Al_2O_3–MgO castables.

Braulio et al. [3–5] and Sako et al. [2] evaluated the effects of silica fume addition in calcium aluminate containing Al_2O_3–MgO castable compositions. This additive is known by its counterbalancing effect on the spinel disruptive expansion due to the softening mechanism associated with generating low melting temperature phases, such as gehlenite or anorthite [3]. Additionally, a further role of SiO_2 in this sort of castable is its ability to speed up $MgAl_2O_4$ formation due to the ion diffusion increase in the presence of liquid phases. Despite these positive aspects, high liquid contents result in shrinkage and decrease refractoriness, directly affecting some of the castable properties, such as the hot modulus of rupture and creep resistance [4].

Refractory castables creep behavior is a key technological issue and the constitutive equations which describe the dependence of deformation (ε) with time (t), applied stress (σ) and temperature (T) could be very useful for evaluating the thermo-mechanical performance of those materials. These relationships are also an important input for finite element analysis used in the stress state calculations of structures in which refractory materials are applied.

The θ-projection concept developed by Evans and Wilshire [6–8] is an alternative to the classical approach to evaluate creep, which is usually based on the steady state analysis. The θ concept considers the ''micro-modeling'' of the dislocation processes that takes place during the primary creep stage and the damage that leads to the strain acceleration in the tertiary one. According to this model, the following constitutive relationship is proposed to describe the creep curve behavior of

* Corresponding author. Tel.: +55 16 33518253; fax: +55 16 33615404.
E-mail address: anapaula.light@gmail.com (A.P. Luz).

0272-8842/$36.00
doi:10.1016/j.ceramint.2011.07.010

brittle materials:

$$\varepsilon = \theta_1(1 - e^{-\theta_2 t}) + \theta_3\theta_4 t, \quad (1)$$

where θi (i = 1, 2, 3 or 4) are the fitting parameters. Parameters θ_1 and θ_2 quantify the total primary strain attained (a condition where the stationary state would eventually be reached) and the curvature of the primary creep stage, respectively. θ_3 and θ_4 characterize the tertiary creep stage. By analyzing other equations used to model the creep deformation-time curve [9], the inverse of θ_2 is equivalent to the so-called "relaxation time" (τ_K). Additionally, the time required to reach the steady state (i.e., ~99% of the time of the total primary strain θ_1) corresponds to $3\tau_K$ and the $\theta_3\theta_4$ parameter is analogue to the creep rate in the secondary stage ($d\varepsilon/dt_{ss}$) [9,10].

The θ approach is suitable to be applied to refractory composition analysis and it does not require the material to reach the steady or secondary state, which is an advantage when compared with the classical evaluation of creep [8]. This method also allows for the interpolation and extrapolation of fitting parameters when time or applied stress or temperature are out of the experimental tested range with higher reliability than the ones attained by other conventional approaches. However, despite these benefits, this calculation procedure has not been extensively applied to the refractory area [7,8].

Considering these aspects, this work addresses the investigation of using the θ-projection concept to calculate and predict the creep behavior of some Al_2O_3–MgO castable compositions containing distinct amounts of silica fume (0–1 wt%). Experimental creep analyses of the designed compositions were carried out at 1450 °C and the attained results were used to calculate the θ_i parameters. Additionally, the effect of the liquid phase formation (derived from the silica fume reactions with the refractory components) on the creep mechanisms were also evaluated by thermodynamic simulations.

2. Experimental

2.1. Materials and experimental tests

Four vibratable alumina–magnesia castables containing different silica fume contents (0, 0.25 0.5 and 1 wt%, 971U, Elkem, Norway) were designed according to the Alfred particle packing model (q = 0.26) [11]. Coarse tabular alumina was added as aggregates ($d \leq 6$ mm, Almatis, USA) and 6 wt% of dead-burnt magnesia ($d < 45$ μm, 95 wt% of MgO, CaO/SiO_2 = 0.37, Magnesita Refratários S.A., Brazil), 7 wt% of reactive alumina (CL370, Almatis, USA), 18 wt% of fine tabular alumina ($d < 200$ μm, Almatis, USA) and 6 wt% of calcium aluminate cement—*CAC*—(Secar 71, Kerneos, France) comprised the matrix of these compositions. The castable dispersion was carried out by adding 0.2 wt% of a polycarboxylate based dispersant (Bayer, Germany), leading to 3.9 wt% water content for a suitable shaping.

Creep tests were performed in a refractoriness under load equipment (Model RUL 421E, Netzsch, Germany). Cylindrical samples (height and external diameter = 50 mm and central inner diameter = 12.4 mm) were prepared according to the 51053 DIN standard, cured at 50 °C, dried at 110 °C for 24 h, followed by calcination at 600 °C and pre-firing at 1550 °C for 24 h. The creep measurements were carried out at 1450 °C for 24 h under a constant compression load of 0.2 MPa. Following that, prismatic samples were prepared (25 mm × 25 mm × 150 mm) and fired at 1150, 1300, 1500 °C for 5 h (heating rate = 1 °C/min) to evaluate the hot (HMOR) modulus of rupture (3-point bending tests) in HBTS 422 equipment (Netzsch, Germany). The HMOR tests were performed at 1150 and 1300 °C for the samples pre-fired at these temperatures, but at 1450 °C for the samples pre-fired at 1500 °C, due to furnace maximum temperature limitation.

2.2. Creep modeling and thermodynamic calculations

The calculation of the θ_i parameters was carried out (based on the experimental creep deformation–time curves) by using the Origin® software (version 8.0724, OriginLab Corporation, USA) and the ExpLinear function. This sort of mathematical fitting comprises the following equation:

$$y = p_1 e^{-x/p_2} + p_3 + p_4 x \quad (2)$$

where p_1, p_2, p_3 and p_4 correspond to θ_1, ${\theta_2}^{-1}$, $-\theta_1$ and $\theta_3\theta_4$, respectively. Additionally, the Origin® software was also used to calculate the linear fitting for the correlation between the θ_i parameters and the silica fume (x_{sf}) or liquid contents (x_L).

Thermodynamic simulations were carried out using FactSage™ [version 6.1, Thermfact/CRCT (Montreal) and GTT-Technologies (Aachen)] in order to predict the castables' phase composition at high temperature (1550 °C). For this study, the databases used were Fact53, SGTE and FToxid, and the Equilib module was selected for the chosen simulations. The calculated chemical compositions of the pre-fired samples were used to better analyze the factors that influence the creep deformation.

3. Results and discussion

3.1. Creep curves

Fig. 1 presents the results of the creep measurements attained for the four designed castable compositions. According to these experimental curves, adding distinct silica fume contents resulted in significant changes in the creep behavior of these refractories and, as observed, the higher the additive content, the higher the material strain is. The curves presented a primary stage and a continuous decrease in the creep rate.

Based on the θ-projection approach, the creep constitutive relationship (Eq. (1)) does not require a steady state condition and, therefore, it can be applied to fit the castable experimental curves evaluated in this work. Following the θ_i parameter calculations, the following equations were attained:

$$\varepsilon = -0.14858(1 - e^{-0.006443t}) - 0.778 \times 10^{-4} t \quad (2)$$

$$\varepsilon = -0.24880(1 - e^{-0.008368t}) - 1.524 \times 10^{-4} t \quad (3)$$

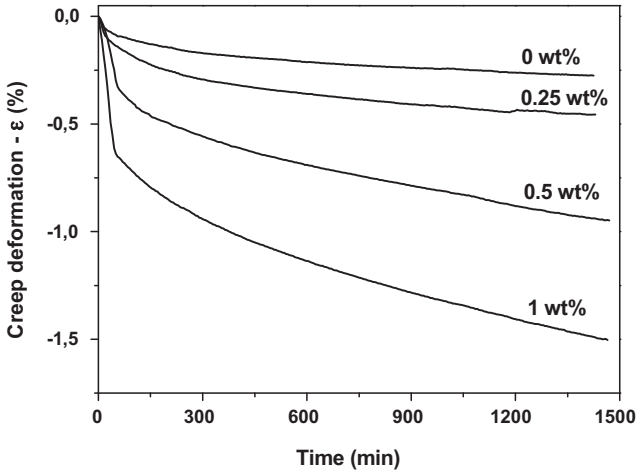

Fig. 1. Creep resistance for the alumina–magnesia castables containing distinct silica fume contents (0, 0.25, 0.5 and 1 wt%) at 1450 °C under a compressive load of 0.2 MPa.

$$\varepsilon = -0.49611(1 - e^{-0.013848t}) - 3.262 \times 10^{-4}t \quad (4)$$

$$\varepsilon = -0.80332(1 - e^{-0.018710t}) - 4.944 \times 10^{-4}t \quad (5)$$

where Eqs. (2)–(5) represent the compositions with 0, 0.25, 0.5 and 1 wt% of silica fume, respectively.

For all tested materials, the fitting of the experimental curves resulted in a very good correlation, with regression coefficient (r^2) values higher than 0.99. Additionally, the error associated with the calculated parameters was lower than 1.2%, 2.5% and 1.5% for θ_1, θ_2 and $\theta_3\theta_4$, respectively. In order to define the dependence of the θ_i parameters on the castables' silica fume content, a second step of the analyses consisted of evaluating the θ_1, θ_2 and $\theta_3\theta_4$ absolute values as a function of the amount of SiO_2 (x_{sf}) added to the compositions (Fig. 2).

The three parameters presented a linear correlation with the silica fume content (Fig. 2) and, as the amount of this additive scales with the maximum primary strain (θ_1), the creep rate moves towards the steady state ($\theta_3\theta_4$). On the other hand, the time required to reach this condition (considered as 3 times the inverse of the θ_2 value) decreases with the increment of silica fume in the castable: 7.8 h > 4.6 h > 3.9 h > 2.6 h for 0, 0.25, 0.5 and 1 wt% of SiO_2, respectively. Thus, based on the maximum primary strain values, as well as the predicted time to reach the secondary creep stage presented above, one can conclude that the steady state should have been reached by the four evaluated refractory materials.

The linear fitting of the θ_i parameters as a function of the silica fume addition (x_{sf}) resulted in r^2 values higher than 0.95 and the following equations were attained (θ_1 and $\theta_3\theta_4$ are presented as absolute values):

$$\theta_1 = 0.12722 + 0.67881x_{sf} \quad (6)$$

$$\theta_2 = 0.00624 + 0.01289x_{sf} \quad (7)$$

$$\theta_3\theta_4 = 7.4x10^{-5} + 4.31x10^{-4}x_{sf} \quad (8)$$

Considering these expressions, the calculation of any other creep deformation–time curve for alumina magnesia castables containing silica fume into the 0–1 wt% range can be carried out with high reliability, without needing additional tests. Fig. 3, for instance, presents the simulated creep curve for a castable with 0.75 wt% of SiO_2 (dashed line). Suitable predictions of the θi parameters and creep curves can also be attained for castable compositions presenting silica fume contents out of the experimental tested range, due to the linear characteristic of Eqs. (6)–(8).

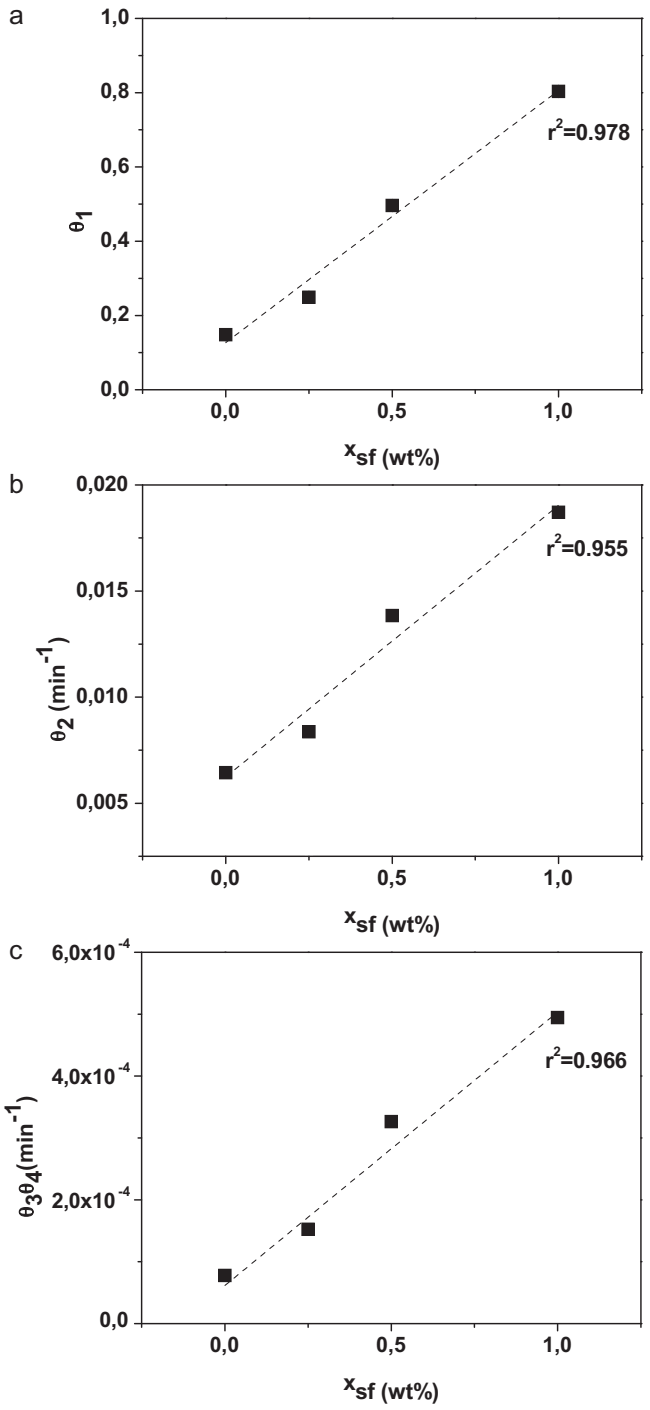

Fig. 2. (a) θ_1, (b) θ_2 and (c) $\theta_3\theta_4$ absolute values as a function of the silica fume content.

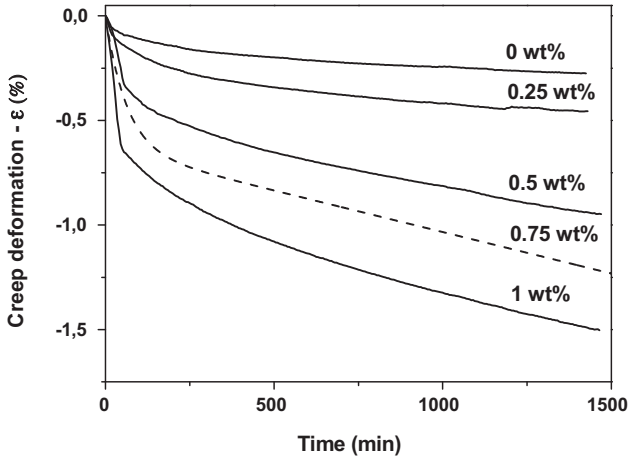

Fig. 3. Experimental (0, 0.25, 0.5 and 1 wt% of silica fume) and simulated creep curves (x_{sf} = 0.75 wt% of silica fume) of alumina–magnesia refractory castables.

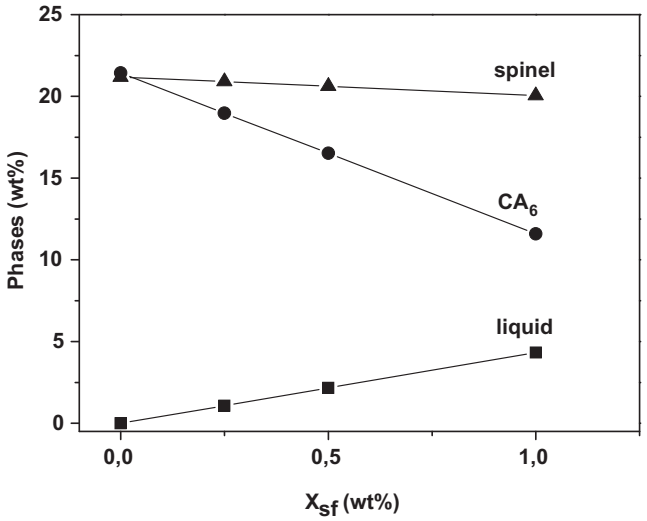

Fig. 4. Calculated compositions of the fired castables attained by thermodynamic simulations (corundum is not presented here, although it is found in the simulations).

However, high silica amounts can result in some major mineralogical and microstructural changes (some of which will be discussed in the next section) in the refractory materials, directly affecting the creep behavior. Thus, despite its expected limitations, the θ approach is a useful tool for the refractory design as it can correlate a compositional variable with a key property (creep resistance) that affects the materials performance in service.

3.2. Creep mechanisms

The creep deformation of the evaluated castables is higher as the silica fume content increases (Fig. 3). However, because the presence of this additive can significantly affect various aspects of the castable microstructure, a systemic analysis is required in order to identify which factors are responsible for controlling the creep behavior of the Al_2O_3–MgO refractories at high temperatures.

In general, the main factors affecting the creep deformation of the refractory materials are: (a) the composition, size and distribution of crystalline aggregates; (b) the degree of direct bonding among different particles, which is associated with the binder phase composition; (c) the content, composition and distribution of fluxes (glassy phases); and (d) the porosity [8,12]. Therefore, in order to understand the creep behavior as a function of the silica fume addition and evaluate the possible phases which have a major impact on the samples deformation, the chemical composition of the designed castables was calculated using thermodynamic software (FactSage^{TM}). The predicted spinel, CA_6 and liquid contents formed at 1550 °C are plotted in Fig. 4 (corundum is not presented in this figure, although it is found in the simulation results).

According to the thermodynamic calculations, the CA_6 formation is reduced by adding higher amounts of silica. Previous investigations [3,5] showed that some differences in the morphology and location of calcium hexaluminate grains were observed by adding silica fume. For example, the silica free castable (0 wt%) displayed equiaxial grains at the edge of tabular alumina aggregates, whereas the refractory containing 1 wt% of this additive presented CA_6 needle-like crystals

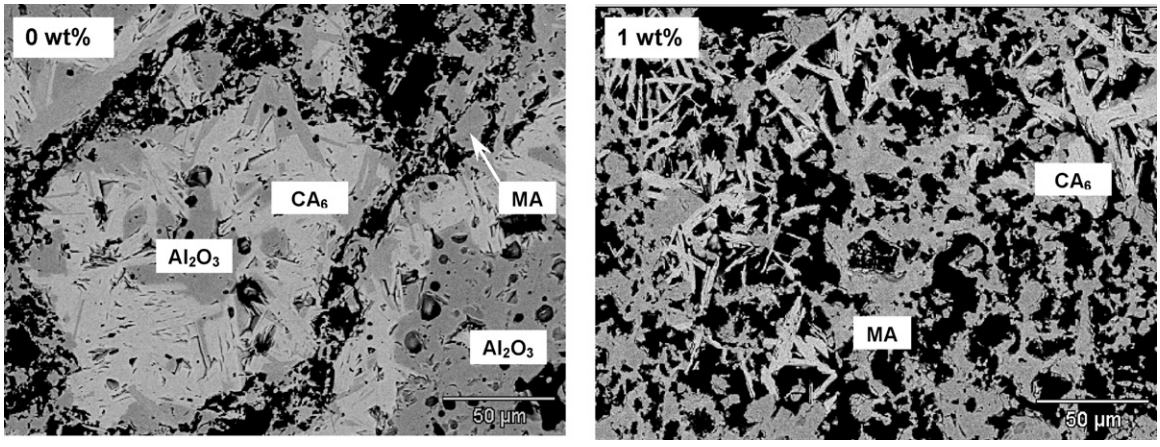

Fig. 5. CA_6 location and morphology in alumina–magnesia castables, containing different silica fume contents (0 and 1 wt%), after firing at 1550 °C for 24 h.

located in the matrix region (Fig. 5). The difference in the crystal shape of this phase was related to the distinct reaction mechanism for its formation: solid state (equiaxial crystal grains) or precipitation from the liquid (acicular grains).

The calcium hexaluminate can play an important role in the refractory creep behavior because its presence as a needle-like phase can induce bridging among the castable particles, resulting in an interlocking effect. Although the needle-like morphology is the most suitable to reduce the creep, these CA_6 crystals were only detected in the samples containing 1 wt% of silica fume, which presented the highest deformation at 1450 °C. Hence, this phase is not pointed out as the major component that affects the performance of these refractories.

Regarding the *in situ* spinel formation, its presence in the castable matrix will generate bonds between the grains. Furthermore, only minor changes in the spinel content (<3 wt%—Fig. 4) are predicted by the simulations for the evaluated castables, indicating that this component does not significantly influence the creep behavior of these materials.

Considering the thermodynamic predictions for the liquid phase, when higher amounts of silica were added to the castables, the liquid content increase was significant (i.e., for the composition with 1 wt% of SiO_2 the liquid content was 3 times higher than for the one with 0.25 wt% of this additive). On the other hand, the composition of this liquid phase was similar for the three silica-fume containing systems: 50.4 wt% of Al_2O_3, 23.1 wt% of SiO_2, 19.1 wt% of CaO and 7.4 wt% of MgO. Based on these results, it can be assumed that the liquid content can be the main factor affecting the creep performance of these materials. This fact is reinforced by its effect on the mechanical strength of the designed castables, as observed by the hot modulus of rupture (HMOR) results presented in Fig. 6. With the increase in the testing temperature and in the silica fume content, the HMOR values tend to decrease based on the liquid amount and its viscosity changes as a function of the temperature.

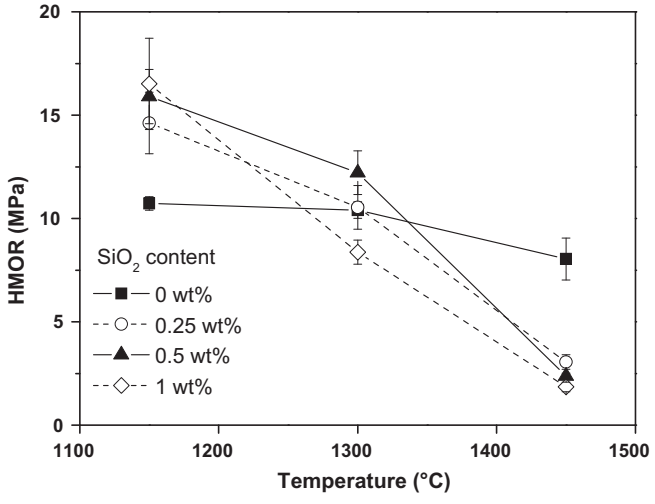

Fig. 6. Hot modulus of rupture (HMOR) at different testing temperatures (1150, 1300 and 1450 °C) for alumina–magnesia castables containing distinct silica fume contents.

Thus, a further analysis was carried out and the creep modeling results (θ_i parameters—Eqs. (6)–(8)) were correlated to those of the thermodynamic simulation (liquid phase content) in order to attain new mathematical expressions for a quantitative evaluation of the castables behavior. The liquid content of the refractories presented a linear correlation with

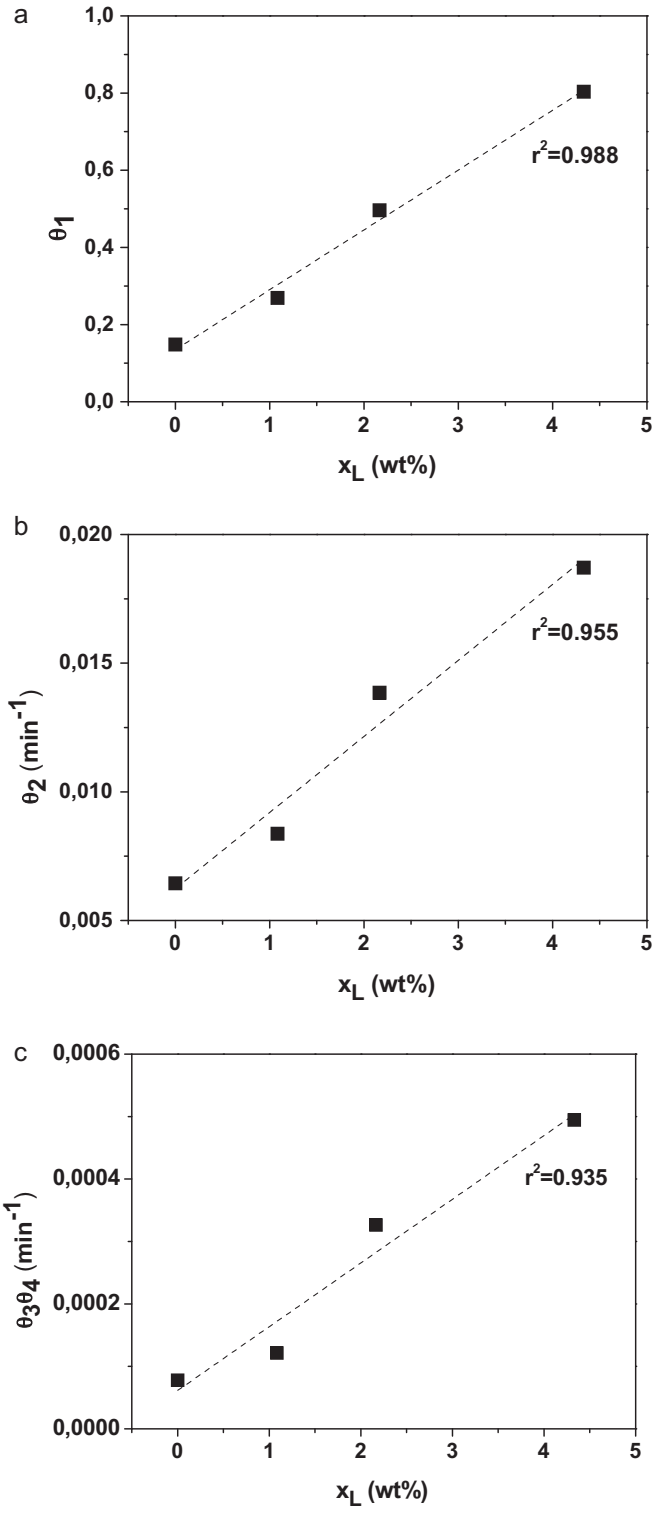

Fig. 7. (a) θ_1, (b) θ_2 and (c) $\theta_3\theta_4$ absolute values as a function of the liquid phase content.

the θ_i parameters (Eqs. (9)–(11)) with regression coefficient values higher than 0.9 (Fig. 7).

$$\theta_1 = 0.13526 + 0.15514x_L \quad (9)$$

$$\theta_2 = 0.00624 + 0.00296x_L \quad (10)$$

$$\theta_3\theta_4 = 6.2 \times 10^{-5} + 1.02 \times 10^{-4}x_L \quad (11)$$

Moreover, the maximum primary strain (θ_1) fitted well with the liquid content results ($r^2 \sim 0.99$), which indicates that the glassy phase of the fired castable should induce the deformation of the samples, mainly at the first creep testing hours at 1450 °C. Considering these aspects, it can be concluded that the main creep mechanism of these Al_2O_3–MgO compositions is related to particles sliding due to the presence of liquid at high temperatures.

The increment in the silica fume content results in higher liquid amounts and: (1) increases the likelihood of liquid distribution around the particles, therefore reducing the direct bonding degree, and (2) increases the viscous phase plastic deformation.

4. Conclusions

Different features can be highlighted by varying the silica fume content, which can be summarized as follows:

- The creep behavior of alumina–magnesia castable scales with the silica fume content.
- A linear dependence of the creep parameters with the silica fume content was attained by modeling the experimental curves using the θ-project concept, which was able to predict the creep performance of other compositions in the same refractory system.
- The silicate glassy phase (which becomes a viscous liquid at high temperatures) was the main factor for the creep behavior and for the decrease in the sample mechanical strength values. This aspect was analyzed by using thermodynamic calculations (liquid content predictions as a function of the silica fume addition) and its correlation with the creep parameters attained using the θ-project concept.
- Analytical expressions able to simulate the refractories creep behavior can reduce the need of additional experimental tests and be an effective tool for the engineered materials design.

Acknowledgments

The authors are grateful to the Federation for International Refractory Research and Education (FIRE), Magnesita Refratários S.A. (Brazil), FAPESP and CNPq.

References

[1] S. Mukhopadhyay, P.K. Das Poddar, Effect of preformed and *in situ* spinels on microstructure and properties of a low cement refractory castable, Ceram. Int. 30 (2004) 369–380.
[2] E.Y. Sako, M.A.L. Braulio, D.H. Milanez, P.O.C. Brant, V.C. Pandolfelli, Microsilica role in the CA_6 formation in cement-bonded spinel refractory castables, J. Mater. Proc. Tech. 209 (2009) 5552–5557.
[3] M.A.L. Braulio, L.R.M. Bittencourt, V.C. Pandolfelli, Microsilica roadmap for alumina magnesia castables expansion, Refract. Appl. News 15 (2010) 12–15.
[4] M.A.L. Braulio, P.O.C. Brant, L.R.M. Bittencourt, V.C. Pandolfelli, Microsilica or MgO grain size: which one mostly affects the *in situ* spinel refractory castable expansion? Ceram. Int. 35 (2009) 3327–3334.
[5] M.A.L. Braulio, L.R.M. Bittencourt, J. Poirier, V.C. Pandolfelli, Microsilica effects on cement conded alumina–magnesia refractory castables, J. Tech. Assoc. Refrac. Jpn. 28 (2008) 180–184.
[6] R.W. Evans, B. Wilshire, Introduction to Creep, The Institute of Materials, London, 1993.
[7] R.W. Evans, B. Wilshire, The theta approach to creep of structural ceramics, Rev. Powder Metall. Phys. Ceram. 5 (1992) 111–168.
[8] R.W. Evans, P.J. Scharning, B. Wilshire, Constitutive equations for creep of a fired doloma refractory, Br. Ceram. Trans. J. 85 (1986) 63–65.
[9] D.J. Bray, Creep of refractories: mathematical modeling, in: R.E. Fisher (Ed.), New Development in Monolithic Refractories–Advances in Ceramics, vol. 13, The American Ceramic society, Columbus, OH, 1995, pp. 69–80.
[10] C. Liu, J.L. Mendoza, R.E. Moore, Effect of stress/strain history on the creep behavior of low cement content refractory concretes, in: R.E. Fisher (Ed.), Advances in Refractories Technology–Ceramic Transactions, vol. 4, The American Ceramic Society, Westerville, OH, 1989.
[11] R.G. Pileggi, A.R. Studart, M.D.M. Innocentini, V.C. Pandolfelli, High performance refractory castables, Am. Ceram. Soc. Bull. 81 (2002) 37–42.
[12] P.J. Dixon-Stubbs, B. Wilshire, High temperature creep behavior of a fired magnesia refractory, Br. Ceram. Trans. J. 80 (1981) 180–185.